

**Supplemental information**

**Functional proteomic profiling links deficient**

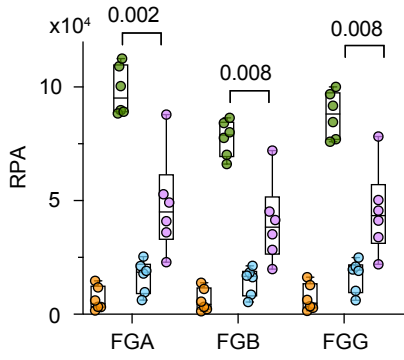
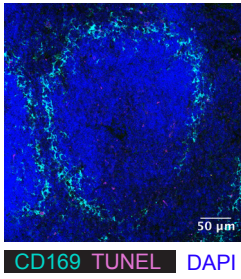
**DNA clearance with increased mortality**

**in individuals with severe COVID-19 pneumonia**

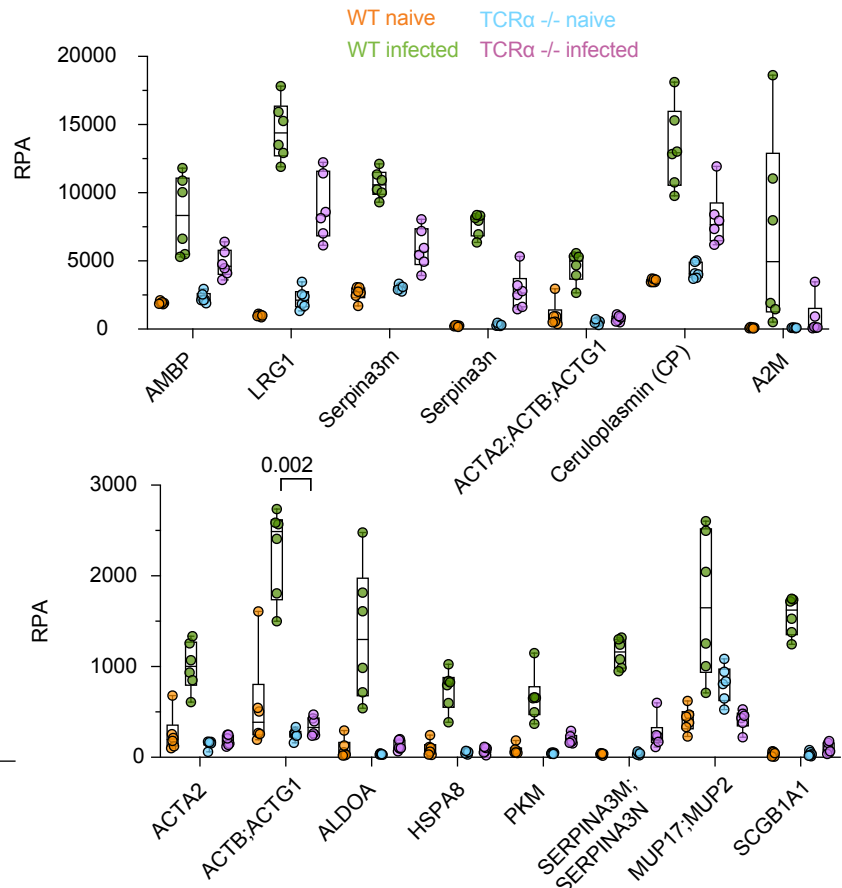
**Iker Valle Aramburu, Dennis Hoving, Spyros I. Vernardis, Martha C.F. Tin, Marianna Ioannou, Mia I. Temkin, Nathalia M. De Vasconcelos, Vadim Demichev, Elisa Theresa Helbig, Lena Lippert, Klaus Stahl, Matthew White, Helena Radbruch, Jana Ihlow, David Horst, Scott T. Chiesa, John E. Deanfield, Sascha David, Christian Bode, Florian Kurth, Markus Ralser, and Venizelos Papayannopoulos**

# Supplemental Figure 1

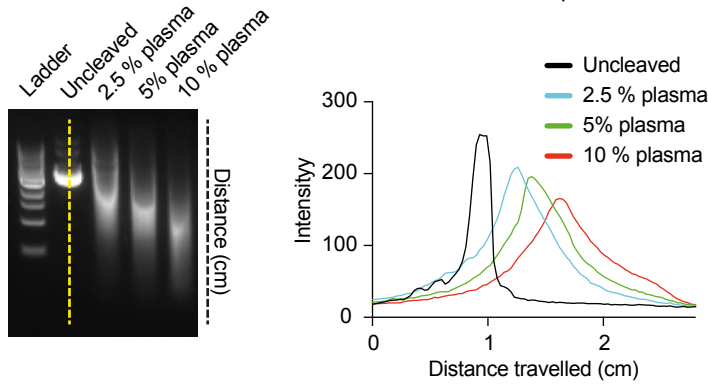
**A**



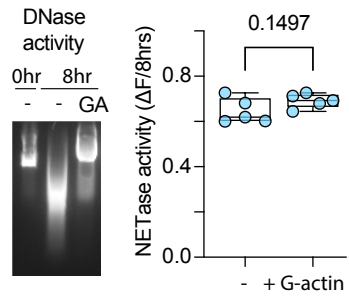
**B**



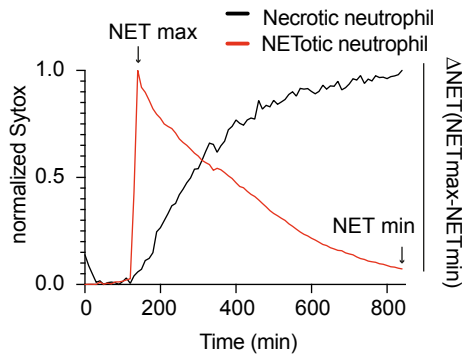
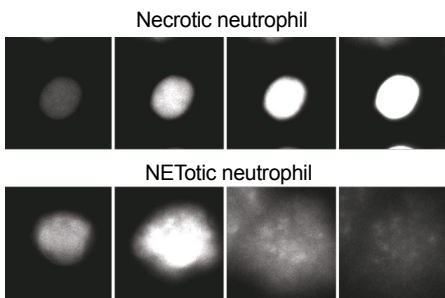
**C**



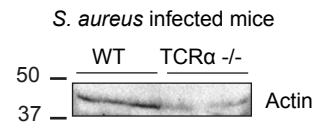
**E**



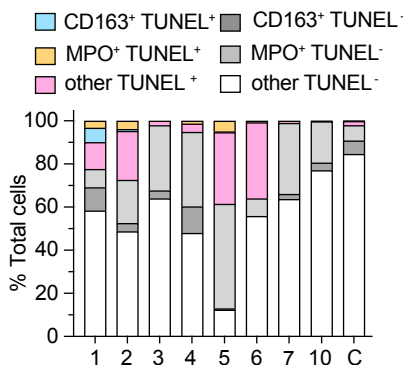
**D**



**F**



**G**



Supplemental Figure 1. T cell death-associated changes in plasma proteins during murine systemic candidiasis. Related to Figure 1.

A. Immunofluorescence confocal micrograph of a naïve WT spleen stained for marginal zone macrophages (CD169; cyan), DAPI (blue) and TUNEL (magenta). Scale bar: 50  $\mu$ m.

B. Relative protein abundance (RPA) of selected proteins in the plasma of WT and TCR $\alpha^{-/-}$  mice, either naïve or infected intravenously with *C. albicans*.

C. Quantification of plasmid DNA degradation by different dilutions of human plasma. Each agarose gel electrophoresis lane was digitally quantified to locate the DNA signal peak and measure the distance travelled (cm).

D. Human neutrophils activated by phorbol 12-myristate 13-acetate (PMA) in the presence of 3% plasma were monitored by time-lapse microscopy for NET degradation measurements. The mean SYTOX fluorescence of each neutrophil was tracked over 12 hrs. Necrotic neutrophils were distinguished from NET-forming neutrophils by the pattern of change in fluorescence (right). NETs dissolved over time leading to a gradual decrease in fluorescence. The fraction of fluorescence loss over time was used to calculate the average mean NET degradation activity for hundreds of NETs per sample.

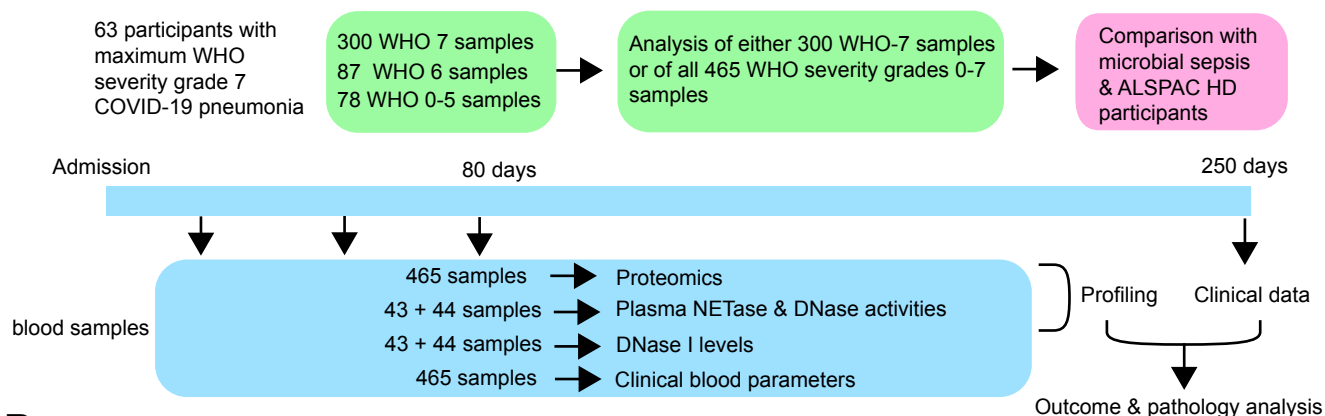
E. Plasmid DNA degradation in healthy plasma alone or in the presence of G-actin (GA) (left). NET degradation in healthy plasma alone or in the presence of G-actin (right).

F. Western blot of actin in plasma of mice infected intravenously with *S. aureus*.

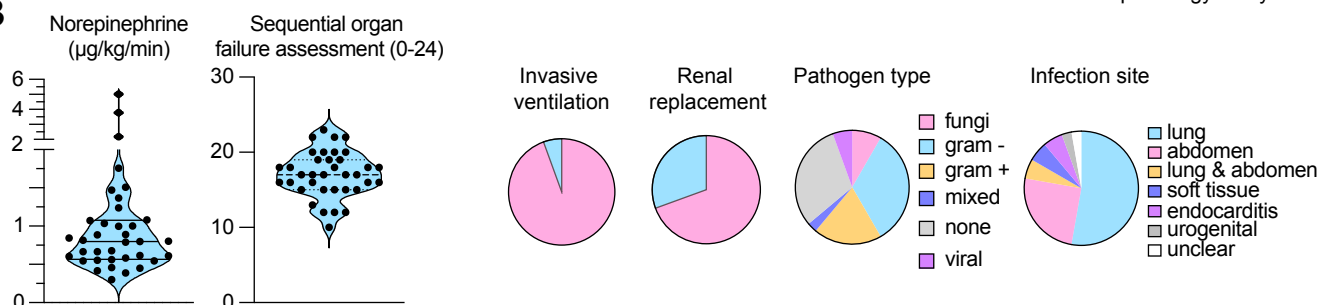
G. Quantification of the percentage of TUNEL<sup>+</sup> and TUNEL<sup>-</sup> cells (grouped for CD163 macrophages, MPO and other cells) from immunofluorescence micrographs of SARS-CoV-2 infected human post-mortem spleens. Statistics by Man-Whitney test for single comparisons.

# Supplemental Figure 2

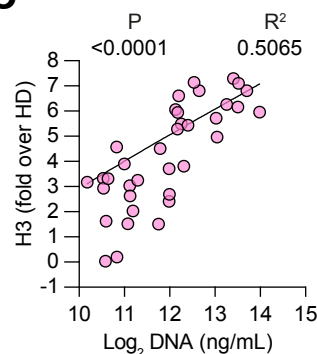
**A**



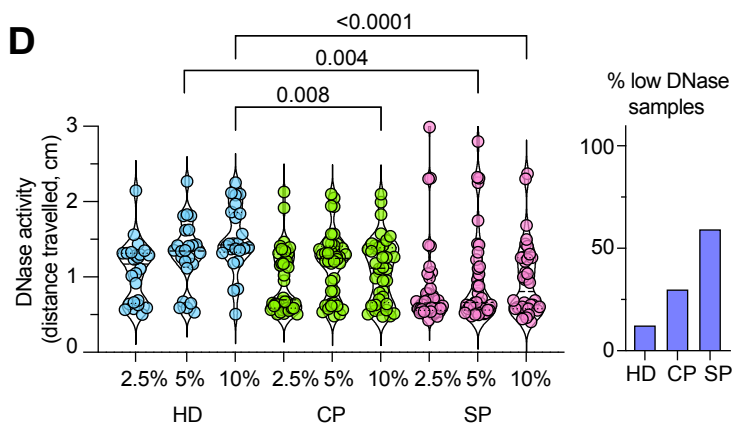
**B**



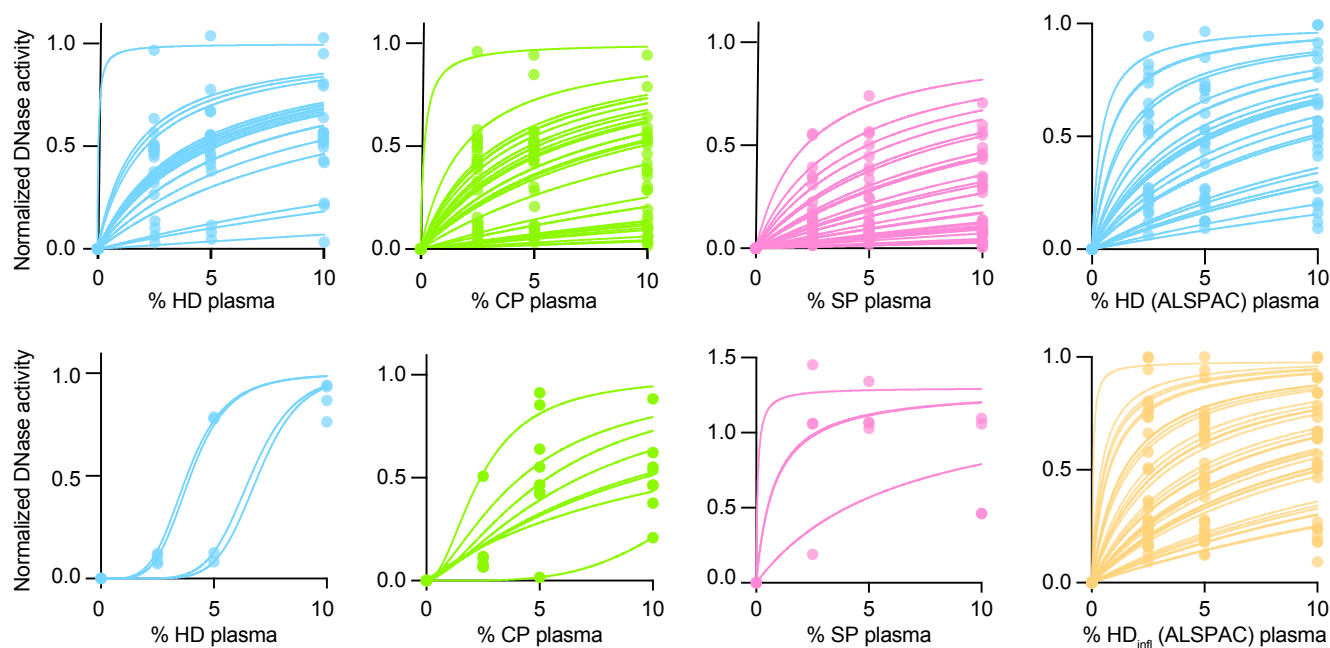
**C**



**D**



**E**



Supplemental Figure 2. Plasma from individuals with sepsis or severe COVID-19 pneumonia exhibit decreased DNA degradation capacity. Related to Figure 2.

A. Scheme illustrating study cohorts, the number of samples analysed and the experimental analysis workflow.

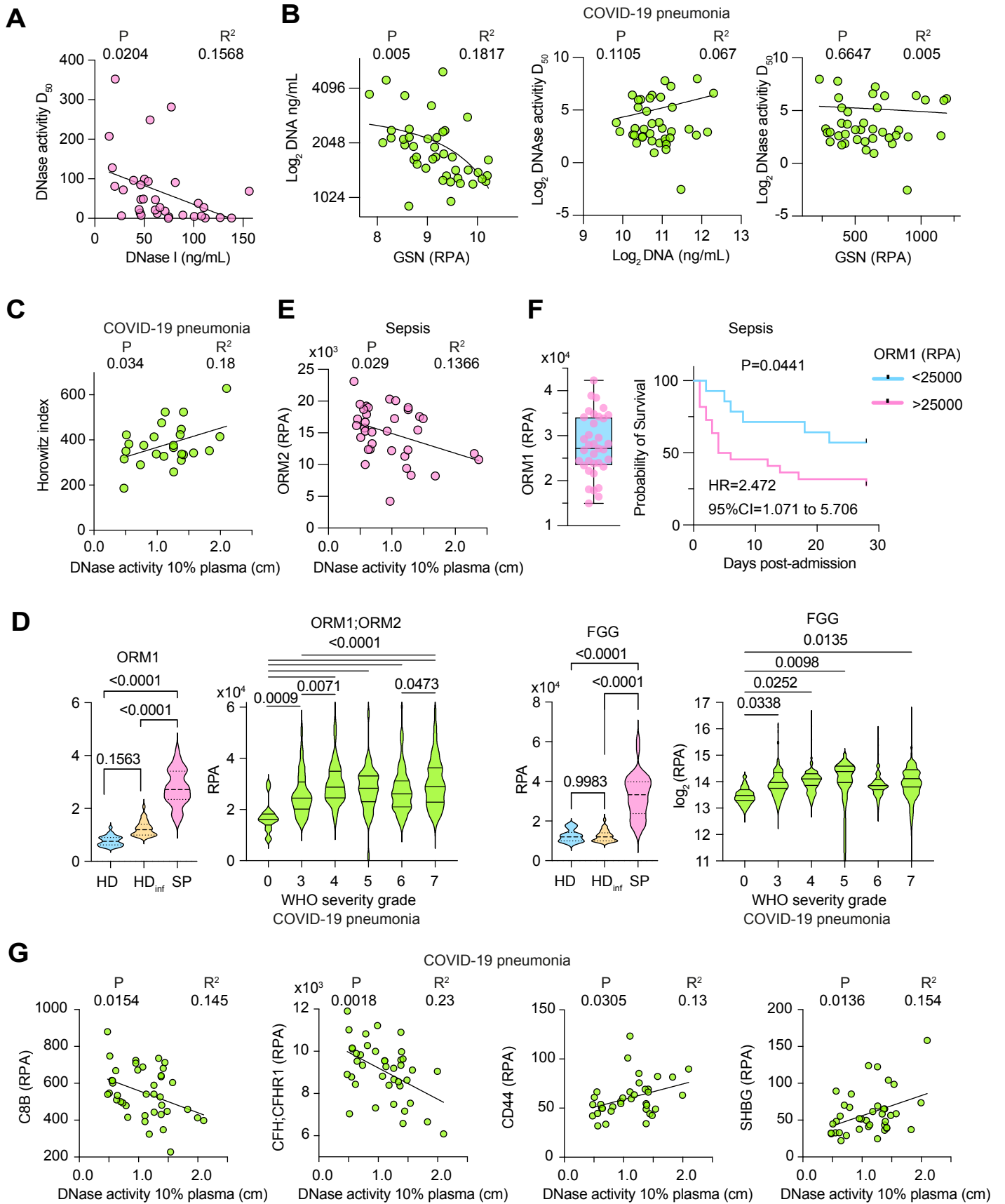
B. Clinical information of the microbial sepsis cohort. Plot indicating the amount of norepinephrine administered and organ failure assessment per participant. The pie charts indicate from left to right, the participants that received invasive ventilation, renal displacements, the type of pathogen identified clinically and the infection site.

C. Correlation between measured extracellular DNA concentration and fold increase in histone H3 protein detected by densitometric analysis of western immunoblots of plasma from individuals with sepsis.

D. DNase activity measured as in (C) in healthy donor (HD), SARS-CoV-2 infected (CP) and microbial sepsis participant (SP) plasmas at 2.5%, 5% and 10% dilution (left). Percentage of low DNase activity samples in HD, CP and SP. Statistical analysis by Kruskal-Wallis test.

E. Best fitting curves for DNase activity values per donor in (C), as well as HD and HD<sub>infl</sub> from the ALPAC study used to calculate the half-maximal activity dilution (D<sub>50</sub>). Curves fitted by non-linear regression to a three-parameter association function.

# Supplemental Figure 3



Supplemental Figure 3. Correlation between DNA degradation activity and the plasma proteome. Related to Figure 3.

A. Correlation between plasma DNase I protein concentration and DNase activity ( $D_{50}$ ) in sepsis participants.

B. Correlation between gelsolin (GSN) relative protein abundance (RPA) and DNA concentration (left), DNase activity ( $D_{50}$ ) and either DNase I (middle) or GSN (RPA) (right) in the plasma of SARS-CoV-2 infected individuals.

C. Correlation between DNase activity in 10% plasma dilution (DNase activity measured as the distance travelled during gel electrophoresis by the substrate DNA after digestion with a 10% dilution of plasma) and the corresponding Horowitz index in WHO severity grade 7 COVID-19 pneumonia plasma samples.

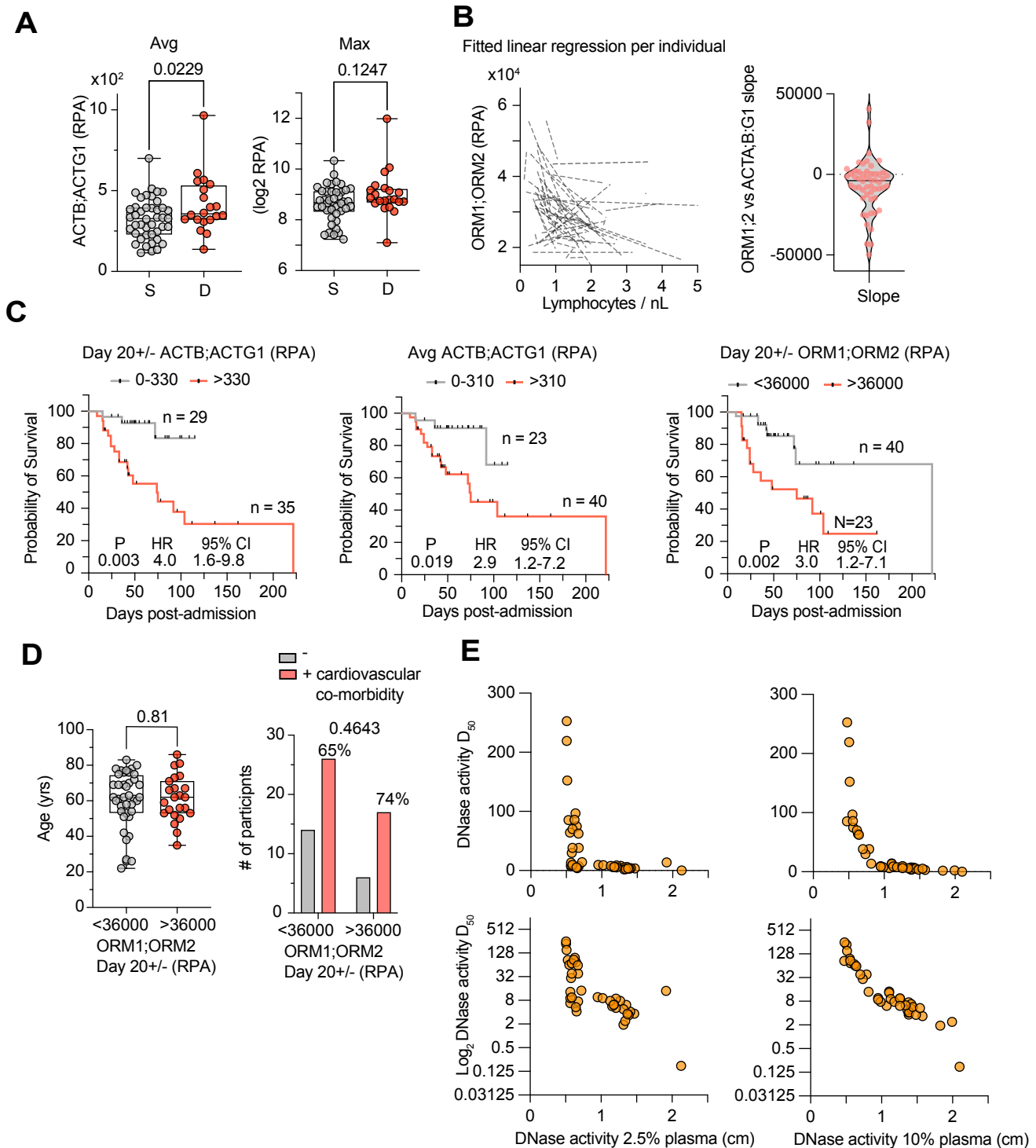
D. Plasma orosomucoid 1 and 2 (ORM1;ORM2) (left) and FGG (right) concentrations in healthy donor (gray) and sepsis (pink) or 687 COVID-19 pneumonia plasma samples (CP, green) segregated by WHO severity grade (right panel).

E. Correlation between DNase activity in 10% plasma dilution and ORM2 levels measured by mass spectrometry in 36 SP plasma samples.

F. ORM1 levels in plasma (left panel) and survival analysis of individuals with microbial sepsis segregated by ORM1 levels either above or below 25000 RPA.

G. Correlation between DNase activity in 10% plasma and complement component C8 beta chain (C8B), complement factor H and CFH-related protein 1 (CFH;CFHR1), CD44 and sex hormone binding globulin (SHBG) in 40 CP plasmas (24 WHO-7, 3 WHO-3 and 13 WHO-4 severity grades) measured by mass spectrometry. Statistics by one-way Anova test for multiple comparisons, and simple linear regression fitting.

# Supplemental Figure 4



Supplemental Figure 4. Relationship of plasma actin and ORM proteins with infection outcome. Related to Figure 4.

A. Average and maximum actin (ACTB;ACTG1) readings per participant with COVID-19 pneumonia (CP) grouped by survival outcome (gray circles for survived and red circles for deceased).

B. Fitted linear regression per participant of ORM1;ORM2 against the corresponding clinical lymphocyte counts per nL (left). Violin plot of each slope in the fitted linear regression analysis (right).

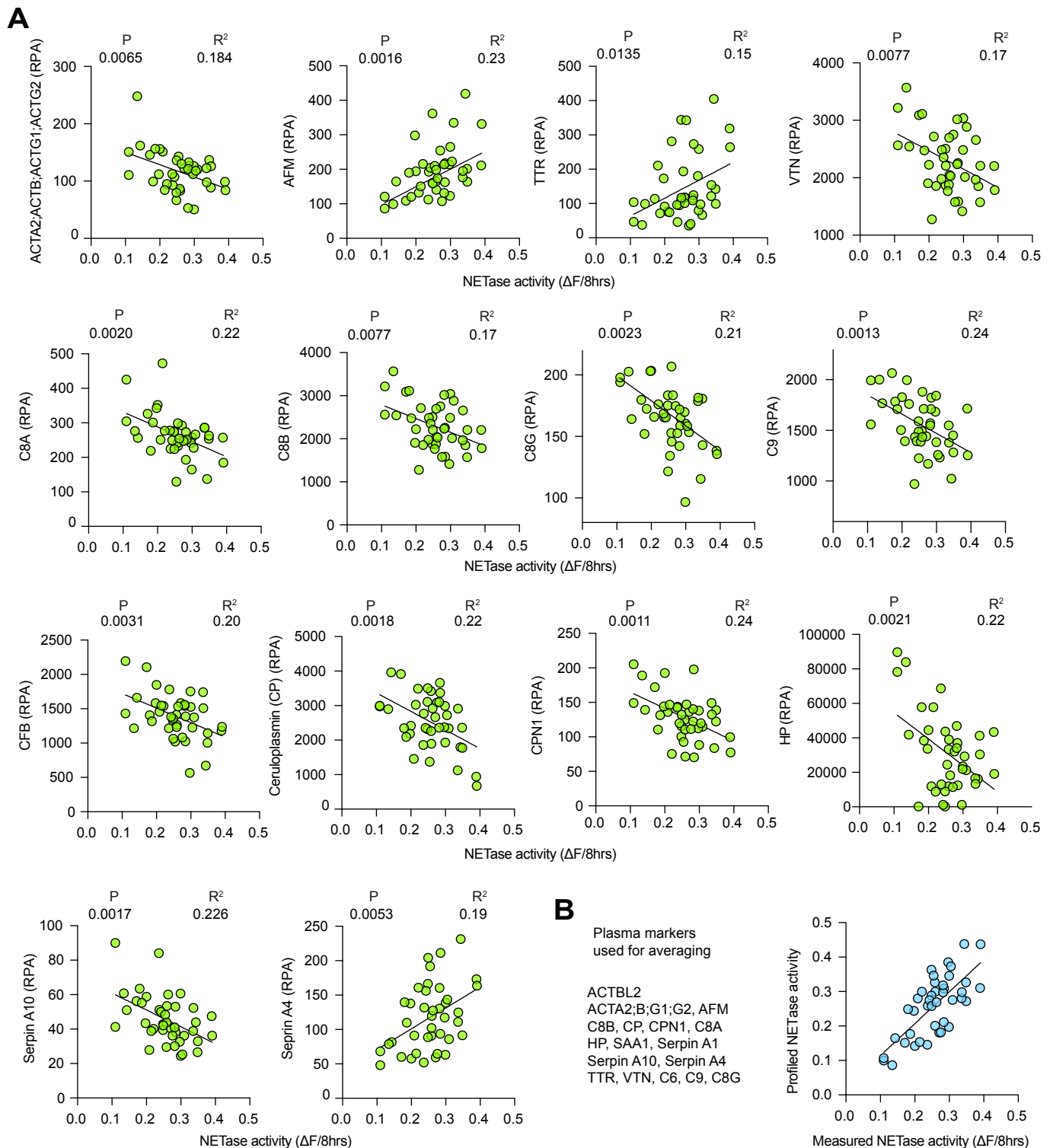
C. Probability of survival in CP clustered into groups according to either their reading proximal to day 20 (Day 20+/-) (left), or longitudinal average ACTB;ACTG1 (middle) or proximal to day 20 (Day 20+/-) ORM1:ORM2 values (right). Black bars indicate censoring events.

D. Age (left) and incidence of cardiovascular co-morbidities (right) in participants grouped according to ORM1;ORM2 values proximal to day 20 (D20+/-) either below 36000 RPA (gray circles) or above 36000 RPA (red circles).

E. Raw DNase activity at 2.5% and 10% plasma dilution plotted against the DNase activity for CP WHO severity grade 7 samples. Statistics by Mann-Whitney test for single comparisons, simple linear regression for fitting or Fisher's exact test for contingency distribution analysis. Survival probabilities calculated by Mantel-Cox survival analysis.



# Supplemental Figure 5

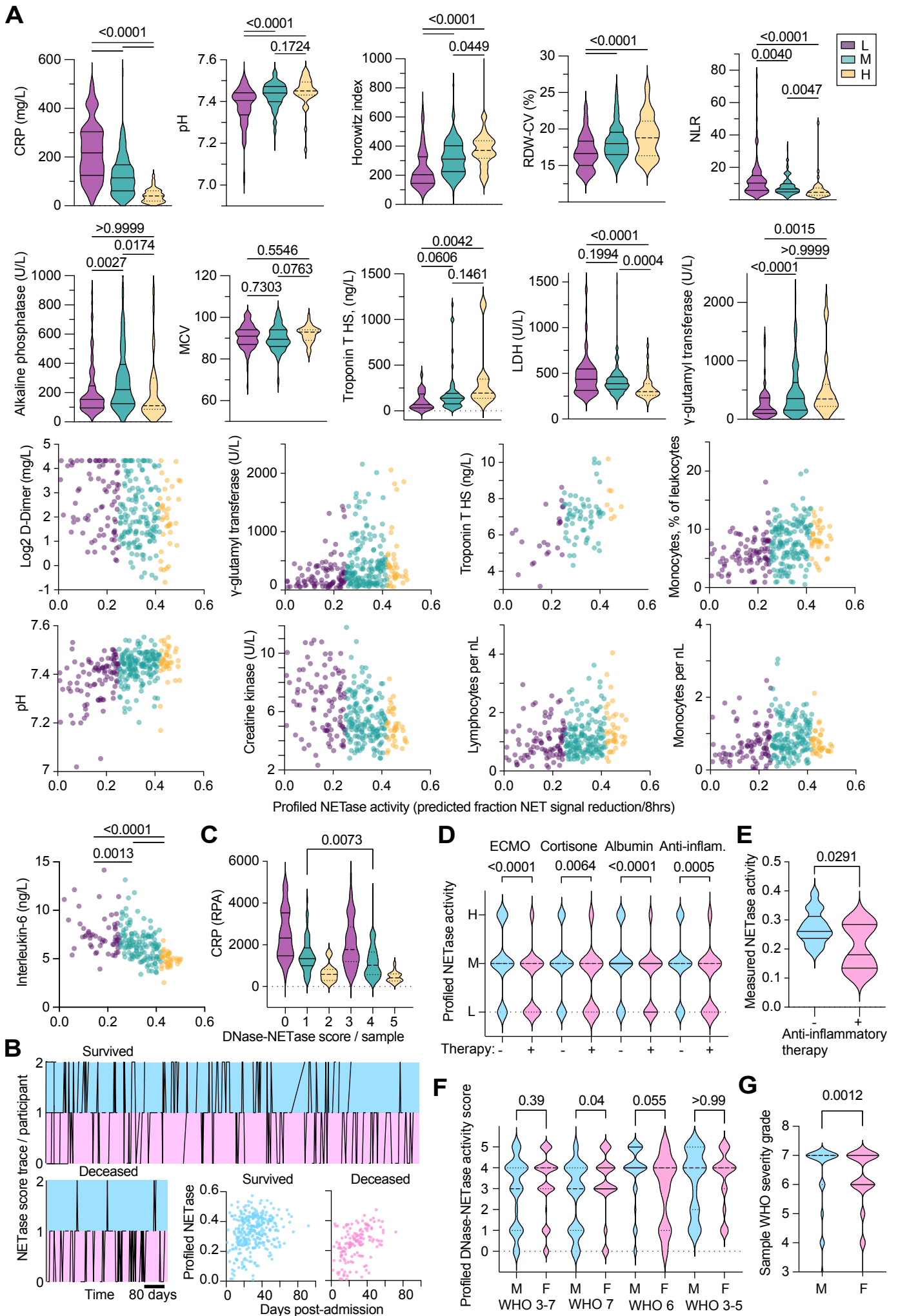


Supplemental Figure 5. Correlation between NETase activity and plasma proteins in participants with COVID-19 pneumonia. Related to Figure 6.

A. A selection of significant correlations between measured NETase activity and the following plasma proteins: actin (ACTA2, ACTB, ACTG1, ACTG2), afamin (AFM), transthyretin (TTR), vitronectin (VTN), complement component C8 alpha chain (C8A), complement component C8 beta chain (C8B), complement component C8 gamma chain (C8G), complement component C9, Complement factor B (CFB), ceruloplasmin (CP), carboxypeptidase N catalytic chain (CPN1), haptoglobin (HP), serpin family A member 10 (SerpinA10), serpin family A member 4 (SerpinA4) in WHO severity grade 7 samples from individuals infected with SARS-CoV-2.

B. Plot of profiled versus measured NETase activity calculated by averaging the predicted NETase values obtained by entering in the corresponding linear fit equations the relative protein abundance of ACTBL2; ACTA2; ACTG1; ACTG2, AFM, C8B, CP, CPN1, C8A, HP, SAA1, Serpin A1, Serpin A10, Serpin A4, TTR, VTN, C6, C9 and C8G. Fitting by simple linear regression.

# Supplemental Figure 6



Supplemental Figure 6. Relationship between NETase activity profiles and clinical markers of severity in COVID-19 pneumonia. Related to Figure 6.

A. Plasma samples from SARS-CoV-2 infected individuals grouped into low (purple) medium (green) and high (yellow) profiled NETase activity and plotted for CRP, Horowitz index, red cell blood distribution width (RDW-CV), neutrophil-to-lymphocyte ratio (NLR), alkaline phosphatase, mean corpuscular volume (MCV), Troponin (TnI), lactate dehydrogenase (LDH), Gamma-glutamyl transferase, D-Dimer, blood monocytes as a % of leukocytes, blood pH, creatine kinase, blood lymphocytes per nL, monocytes per nl and IL-6.

B. Individual longitudinal NETase score trace of all WHO severity samples per participant over the time of collection, segregated by survival outcome. The profiled NETase values of each sample over time plotted by survival outcome (lower right insert graphs).

C. Plasma CRP relative protein abundance in samples grouped by the combined profiled DNase and NETase activity score.

D. Low (L), medium (M) or high (H) profiled NETase activity in CP samples grouped by whether the participants were receiving extracorporeal membrane oxygenation ECMO, hydrocortisone, albumin or anti-inflammatory therapy at the time of collection.

E. Measured NETase activity of samples segregated by whether the participants were receiving anti-inflammatory therapy at the time of sample collection.

F. Combined profiled DNase and NETase activity score segregated by donor sex and WHO severity.

G. Distribution of WHO severity grade classification of samples from male and female SARS-CoV-2 infected individuals. Statistics by one-way Anova or Kruskal-Wallis tests.

